

Steady-State Motion of a Liquid/Liquid/Solid Contact Line

JEAN-FRANÇOIS JOANNY* AND DAVID ANDELMAN†¹

**Département de Physique des Matériaux, Université C. Bernard—Lyon I, 69622 Villeurbanne Cedex, France;*
†*Corporate Research Science Laboratories, Exxon Research and Engineering Company, Annandale, New Jersey 08801; and †Physique de la Matière Condensée, Collège de France, 75231 Paris Cedex 05, France*

Received August 12, 1986; accepted November 19, 1986

The steady-state motion of a liquid A/liquid B interface on a flat solid surface is investigated. Hydrodynamic equations for the flow are obtained and in principle could yield a solution for the profile of a general curved A/B interface. For small contact angles this problem is quite similar to the dynamics of a liquid/vapor/solid contact line. We consider both a "dry" solid surface and one that has been prewetted by an invading liquid. Interesting Saffman-Taylor-like instabilities could appear close to the tip of the advancing contact line for appropriate viscosity ratios. © 1987 Academic Press, Inc.

I. INTRODUCTION

The dynamics of motion of the three-phase contact line has received much attention over the last few years (1, 2), mainly due to the apparent incompatibility between the advancing motion of the liquid and the *no-slip* boundary condition at the solid surface.

One of the ideas proposed to resolve this contradiction was to allow a small slip velocity of the advancing liquid at the solid surface. This idea, although successful from a mathematical point of view, is not well justified from a physical point of view, except in the case of polymeric liquids of high molecular weight. There, the presence of entanglements causes a *plug flow*; hence entangled polymeric liquids behave as solids and therefore have a finite slip velocity on the solid surface. Brochard and de Gennes (3) have explained in this way the special features of polymeric liquid spreading: the appearance of a "foot" at the edge of the spreading liquid.

Nevertheless, this mechanism of entanglement is not present for simple liquids, where a slip boundary condition cannot be understood physically. There, it was found quite re-

cently (4, 5) that long-range molecular forces (mainly van der Waals forces) play an important role for very thin liquid films, i.e., at the edge of an advancing liquid.

A considerable amount of work has been devoted to the spreading of a nonvolatile liquid surrounded by a vapor phase. In this situation two regions can be distinguished in the advancing liquid front:

(1) A *macroscopic wedge* characterized by an apparent (dynamic) contact angle θ_d which depends on the advancing velocity u , the liquid/vapor interfacial tension γ , and the liquid viscosity η , through Tanner's law (6)

$$\theta_d^3 \simeq \frac{\eta u}{\gamma} \quad [1]$$

(2a) On a dry solid (with no preexisting liquid film), Fig. 1, a thin *precursor film* advances ahead of the macroscopic front. The minimum thickness e and the length l of this precursor film (4, 7) depend mainly on the spreading power S which is the difference in interfacial tensions,

$$S = \gamma_{SV} - \gamma - \gamma_{SL} > 0, \quad [2]$$

where γ_{SV} and γ_{SL} are the solid/vapor and solid/liquid interfacial tensions, respectively.

¹ To whom correspondence should be addressed.

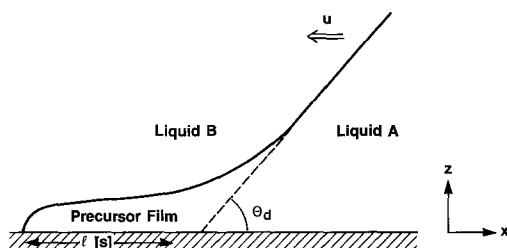


FIG. 1. Dry wetting: the macroscopic wedge of liquid A is advancing at a constant velocity u on a solid surface into an external liquid B. The dynamic contact angle is θ_d and the wedge is preceded by a precursor film of length $l(S)$.

Since it is a complete wetting situation, $S > 0$, and

$$e(S) = a \left(\frac{3\gamma}{2S} \right)^{1/2}, \quad l(S) = \frac{a^2}{e\theta_d^3}, \quad [3]$$

a being the molecular length.

(2b) On a solid already wetted by a preexisting liquid film, the macroscopic wedge crosses over smoothly to this preexisting film (5, 8).

The problem of the no-slip boundary condition at the actual contact line (at the "tip" of the precursor film), Fig. 1, is then solved by itself, since the local contact angle (to be distinguished from the apparent contact angle, θ_d) has a value of $\pi/2$. This allows the spreading motion with a no-slip boundary condition at the solid surface. Experimentally, the macroscopic law, Eq. [1], seems well verified for silicon oils (6) and the existence of the precursor film has been known for quite a long time (9). However, some more quantitative experiments are needed, especially in the microscopic region described above.

In what follows, we address the problem of the dynamics of a liquid A/liquid B/solid contact line. This is a generalization of the liquid/vapor/solid problem and is of considerable interest in the field of surface chemistry. Experiments where another immiscible liquid is used as the external phase (and not the vapor) might eliminate some of the difficulties associated

with a liquid/vapor front, such as mechanical vibration, contamination from the external phase, and evaporation and recondensation of the liquid which is volatile to some extent. However, one must consider in addition the effects of a nonnegligible viscosity of the external liquid.

In this paper, we show that in the limit of small contact angles, θ_d (i.e., at later stages of the spreading) the spreading dynamics of a liquid depends only weakly on the viscosity of the external liquid, for viscosities that are not too large. For small dynamic contact angles, the velocity gradients in the spreading liquid are very large and most of the viscous dissipation occurs in that liquid.

Very few theoretical studies addressed the problem of the dynamics of the liquid A/liquid B/solid contact line. Huh and Scriven (1) assume that the liquid A/liquid B interface is a perfect rigid wedge with a given contact angle θ . Consequently, they derive the solution of the hydrodynamic equations as a function of this angle θ and the viscosities of the two incompressible liquids.

Pumir and Pomeau (10) propose a scaling form for the hydrodynamic stress tensor at the liquid A/liquid B interface and then qualitatively study the shape of this interface. They predict corrugations of the interface with dilatational invariance in a two-dimensional geometry.

Our approach lies somewhere in between; in the limit of small contact angles we solve, in Section II, the flow equation in the external phase. We are then left with an integro-differential equation for the inner liquid wedge. Its solution can, in principle, give the exact shape of the A/B interface, without having to presume that it is a rigid wedge, as was assumed in Ref. (1). We obtain only an approximate solution of this integro-differential equation, and in the limit of small contact angles we get the first correction to the velocity profile in the inner phase. Our solution *does not* show any major differences with the liquid/vapor/solid problem. Both "dry" and prewetted surfaces are studied in Section III; in addition,

the flow field lines are quite similar to the ones calculated by Huh and Scriven (1). Our conclusions are presented in Section IV, where we discuss qualitatively larger contact angles for which corrugation of the interface might appear. The possibility of an instability of the three-phase contact line is also proposed. It resembles the viscous fingering instability (11) in a Hele–Shaw geometry.

II. HYDRODYNAMIC EQUATIONS

The geometry of the problem is sketched in Fig. 1, where for simplicity we look at a two-dimensional geometry. The inner liquid A has a viscosity η_{in} and the external liquid B has a viscosity η_{ex} . We are interested in the steady-state motion where the advancing velocity u is constant. All our results will be presented in a reference frame for which the solid surface is stationary. [In Ref. (1), the reference frame is moving with velocity $-u$ and the liquids are stationary.]

1. The External Liquid Phase

A simple solution of the flow equation in the external liquid is obtained if we assume that for the external liquid, the A/B interface lies on the x -axis ($z = 0, x > 0$). This is a good approximation for small contact angles, $\theta_d \ll 1$. The velocity on the interface, $V(x)$, is then parallel to the solid surface (the x -axis). The flow equation in the external liquid can be derived from the Navier–Stokes equation for incompressible liquids. It is convenient to introduce the stream function, $\Psi(x, z)$, which is related to the velocity components by

$$\begin{aligned} v_x &= \frac{\partial \Psi}{\partial z}, \\ v_z &= -\frac{\partial \Psi}{\partial x}. \end{aligned} \quad [4]$$

In the limit of small advancing velocities, the stream function satisfies a biharmonic equation (1)

$$\nabla^2(\nabla^2 \Psi) = 0, \quad [5]$$

with the following boundary conditions:

- (i) $v_z = 0$ on the solid surface, $z = 0$.
- (ii) No-slip boundary condition: $v_x = 0$ on the solid surface ($z = 0, x < 0$).
- (iii) No-slip boundary condition: $v_x = V(x)$ at the A/B interface ($z = 0, x > 0$).
- (iv) The velocity is bounded at infinity.

The Fourier transform in the x -variable of the stream function, $\tilde{\Psi}(q, z) = \int e^{-iqx} \Psi(x, z) dx$, can be expressed in terms of the Fourier components of the velocity at the interface, $\tilde{V}(q)$,

$$\tilde{\Psi}(q, z) = \tilde{V}(q) z e^{-|q|z}, \quad [6]$$

and the velocity in the external liquid is then given by

$$\begin{aligned} \tilde{v}_x(q, z) &= \tilde{V}(q) [1 - |q|z] e^{-|q|z}, \\ \tilde{v}_z(q, z) &= -i \tilde{V}(q) |q| z e^{-|q|z}. \end{aligned} \quad [7]$$

The Fourier transform of the pressure, $\tilde{P}(q, z)$, can then be calculated through the Navier–Stokes equation

$$\tilde{P}(q, z) = -2i |q| \eta_{ex} \tilde{V}(q) e^{-|q|z}. \quad [8]$$

Finally, the Fourier transform of the hydrodynamic stress tensor,

$$\sigma_{ij} = -P \delta_{ij} + \eta_{ex} \left(\frac{\partial v_i}{\partial x_j} + \frac{\partial v_j}{\partial x_i} \right),$$

is obtained from Eqs. [7] and [8], where x_i ($i = 1, 2$) stands for x and z , respectively,

$$\begin{aligned} \tilde{\sigma}_{ij}(q, z) &= \eta_{ex} \tilde{V}(q) e^{-|q|z} \begin{pmatrix} 2i |q| (2 - |q|z) & -2 |q| + 2q^2 z \\ -2 |q| + 2q^2 z & 2i q^2 z \end{pmatrix} \end{aligned} \quad [9]$$

Equations [7]–[9] completely characterize the flow in the external liquid B as a function of the velocity at the interface, $V(x)$. This velocity is obtained in the next section by calculating the flow in the inner advancing liquid A and by matching boundary conditions on the A/B interface.

2. The Inner Liquid Phase

For the inner phase, even in the limit of small contact angles, $\theta_d \ll 1$, the profile of the A/B interface, $\zeta(x)$, cannot be set to zero (as was done for the external liquid). Rather, its shape and the velocity profile of the inner liquid should be determined self-consistently. Our approach is to use the lubrication approximation (12) in order to get the flow equations in the inner liquid,

$$\eta_{in} v_x(z) = \frac{1}{2} \frac{\partial P}{\partial x} z^2 + bz, \quad [10]$$

where $\partial P/\partial x$ is the pressure gradient in the inner liquid A and is z -independent in the lubrication approximation (12). The pressure P itself is related to the component σ_{zz} of the stress tensor on the boundary of the external liquid B, $z = 0$, by the Laplace equation

$$P(x) = -\sigma_{zz}(z=0) - \gamma \nabla^2 \zeta(x) = -\gamma \nabla^2 \zeta(x),$$

where again the difference between the x -axis and the A/B interface is neglected for the external liquid in the limit of small contact angles, and $b(x)$ is an integration constant (of the z -variable) to be determined below.

The continuity of the tangential component of the stress tensor, σ_{xz} , at the A/B interface fixes the integration constant b ,

$$b = \sigma_{xz}(x, z=0) - \frac{\partial P}{\partial x} \zeta. \quad [11]$$

In addition, $v_x(\zeta) = V(x)|_{z=0}$ at the interface; thus Eqs. [8]–[11] relate the interface velocity $V(x)$ to the tangential component of the stress tensor $\sigma_{xz}(x)$ at the interface

$$\eta_{in} V(x) = -\frac{1}{2} \frac{\partial P}{\partial x} \zeta^2(x) + \sigma_{xz}(x) \zeta(x),$$

$$\sigma_{xz}(x) = \frac{2}{\pi} \eta_{ex} \int_{-\infty}^{+\infty} \frac{V(x')}{(x-x')^2} dx'. \quad [12]$$

Note that the integral in Eq. [12], which was obtained by the inverse Fourier transform of Eq. [9], is the *Cauchy principal part*; thus, it is well defined.

The average velocity

$$u = \zeta^{-1} \int_0^\zeta v_x(z) dz$$

is obtained by averaging the lubrication equation [10] over the thickness $\zeta(x)$,

$$\eta_{in} u = -\frac{1}{3} \frac{\partial P}{\partial x} \zeta^2(x) + \frac{1}{2} \sigma_{xz}(x) \zeta(x). \quad [13]$$

It is convenient to introduce an excess velocity, $\omega(x) \equiv V(x) - 3u/2$ instead of $V(x)$.

The excess velocity $\omega(x)$ and the tangential stress component, σ_{xz} , Eqs. [12] and [13], are related by two simpler equations

$$\eta_{in} \omega(x) = \frac{1}{4} \sigma_{xz}(x) \zeta(x),$$

$$\omega(x) = \frac{1}{2\pi} \frac{\eta_{ex}}{\eta_{in}} \zeta(x) \int_{-\infty}^{+\infty} \frac{\omega(x')}{(x-x')^2} dx', \quad [14]$$

where again the integral in the last equation is the Cauchy principal part.

The solution of Eq. [14] and then Eq. [13] gives the profile of the advancing liquid interface. We now study this profile in two situations:

- (i) When the solid surface is initially covered only with the external liquid B (“dry” wetting), Fig. 1.
- (ii) When the solid was previously wetted by a thin layer of the inner liquid A (“moist” wetting), Fig. 2.

The terminology “dry” and “moist” is given in analogy with the liquid/vapor case where the external liquid is the vapor.

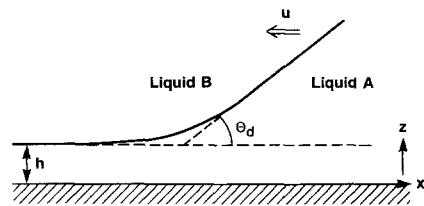


FIG. 2. Moist wetting: as in Fig. 1, but the solid is already covered by a film of thickness $z = h$ of liquid B (before the spreading of liquid A).

III. THE LIQUID A/LIQUID B INTERFACE PROFILE

1. Dry Wetting

In the case of dry wetting, Fig. 1, the solid is entirely covered with liquid B before the spreading of liquid A. The advancing velocity u is a constant. Part of the solid (all the region, $x < 0$) is still covered by liquid B. For $x < 0$ and $z = 0$, the no-slip boundary condition imposes

$$V(x) = 0 \quad \text{or} \quad \omega(x) = -\frac{3}{2}u \quad \text{for } x < 0. \quad [15]$$

It is extremely difficult to solve Eq. [14] exactly because of the singular kernel in the integral. Instead, as a first approximation, we neglect in Eq. [14] the excess velocity at the interface ($x > 0$), $\omega(x) = 0$. This leads to a simplified equation for the profile,

$$\eta_{in}u + \frac{1}{3}\zeta^2 \frac{\partial P}{\partial x} + \frac{3}{2\pi}\eta_{ex}u \frac{\zeta}{x} = 0. \quad [16]$$

We note that this equation has the same structure as that proposed by Pumir and Pomeau (10). However in the limit of small dynamic contact angle, $\theta_d \ll \eta_{in}/\eta_{ex}$, the viscous friction in the external liquid (the third term in Eq. [16]) is small compared to the viscous friction in the inner liquid (first term in Eq. [16]) and one can thus neglect viscous dissipation in the external liquid as in the liquid/vapor case.

Within this approximation [$V(x) = 0, x < 0$; $V(x) = 3u/2, x > 0$] we can calculate the stream function in the external liquid using Eq. [6],

$$\Psi(x, z) = \frac{3u}{2\pi}z \operatorname{tg}^{-1}\left(\frac{x}{z}\right) + \frac{3}{4}uz, \quad [17a]$$

or in polar coordinates (r, Φ)

$$\Psi(r, \Phi) = \frac{3u}{2\pi}r(\pi - \Phi)\sin \Phi. \quad [17b]$$

Equation [17b] is related to the flow-field equation derived by Ref. (1) for a perfect rigid wedge in the limit of small wedge angle, $\theta \ll \eta_{in}/\eta_{ex}$. Their flow field is exactly

$$\Psi = ur \sin \Phi,$$

where the additional term expresses a different choice of a reference frame; theirs moves with velocity u with respect to ours. In Fig. 3, lines of constant stream field are shown for three cases: $\Psi/u = 3, \frac{3}{2},$ and $\frac{3}{4}$.

A better solution of Eq. [14], which is self-consistent for $\omega(x)$, can be obtained by neglecting the variation with x of $\theta_d = \zeta/x$ in Eq. [14],

$$\omega(x) = -\frac{3}{1 + \frac{1}{2\pi} \frac{\eta_{ex} \zeta}{\eta_{in} x}} \frac{\eta_{ex} \zeta}{\eta_{in} x} u \quad x > 0,$$

$$\omega(x) = -\frac{3}{2}u \quad x < 0. \quad [18]$$

The equation that gives the interface profile is then derived from Eqs. [13] and [18],

$$\eta_{in}u = -\frac{1}{3}\zeta^2 \frac{\partial P}{\partial x} - \frac{3}{2\pi} \frac{\frac{\zeta}{x}\eta_{ex}}{1 + \frac{1}{2\pi} \frac{\eta_{ex} \zeta}{\eta_{in} x}} u. \quad [19]$$

We can further distinguish two limits:

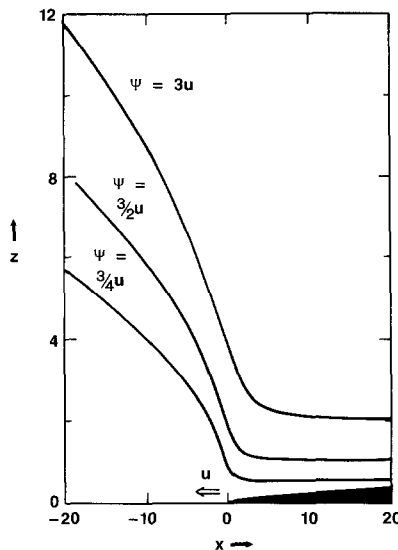


FIG. 3. Flow lines in the external liquid phase as determined from Eq. [17a] in the limit $\theta_d \ll \eta_{in}/\eta_{ex}$. The liquid A/liquid B interface is shown schematically. Three flow lines with $\Psi/u = 3, 3/2, 3/4$ are shown.

(i) In the limit where $\theta_d \ll \eta_{in}/\eta_{ex}$, Eq. [19] reduces to Eq. [16]. Note that this particular limit can be more restrictive than the general limit of small contact angles, $\theta_d \ll 1$. The velocity $\omega(x)$ can then be neglected on the interface $\zeta(x)$ for $x > 0$.

(ii) Another special case is the case of very viscous external liquid (e.g., for a polymeric oil). In this case we may have $\theta_d \gg \eta_{in}/\eta_{ex}$, even though $\theta_d \ll 1$. The interface profile is then obtained from Eq. [19],

$$\eta_{in} u = -\frac{1}{12} \zeta^2 \frac{\partial P}{\partial x}. \quad [20]$$

We note that Eq. [20] is similar to the equation for the liquid/vapor interface profile with the only difference that the numerical prefactor $\frac{1}{12}$ replaces the usual $\frac{1}{3}$. This correction is easily understood if we consider an external liquid with infinite viscosity, $\eta_{ex} = \infty$; this "liquid" behaves as a solid and Eq. [20] is then exactly the Poiseuille equation for a viscous liquid moving between two parallel plates which are at a distance ζ from one another.

The introduction of viscous dissipation, Eq. [16], in the external liquid phase does not eliminate the problem of the moving contact line. (Equation [16] does not have any solution with $\zeta = 0$ at finite x .) The solution to this problem is to consider the effect of long-range (e.g., van der Waals) forces which are important close to the contact line; this was applied successfully to the liquid/vapor case (2, 4, 5). Here as well, they are responsible for the existence of a precursor film which moves ahead of the macroscopic wedge. The profile of the precursor film can be determined by neglecting viscous dissipation in the external liquid (this approximation is even better justified for the precursor film than for the macroscopic wedge since the effective contact angle, $\theta_d \cong 0$, in the film); hence its thickness $e(S)$ and its length $l(S)$ are still given by Eq. [3].

It should also be noted that the existence of the precursor film further reduces the dissipation in the external liquid. The nominal contact line is not at $x = 0$ (the position of the

apparent macroscopic wedge in the moving reference frame), but at $x = -l$. The excess velocity $\omega(x)$ in the precursor film is, in a first approximation, also zero if $x > -l$ and is given by Eq. [18] for $x < -l$. One should thus replace ζ/x by $\zeta/(x + l)$ in Eq. [16].

2. Moist Wetting

In this case, before the spreading of liquid A, the solid is already covered with a thin film of liquid A of thickness h , as is shown in Fig. 2. The advancing velocity is not the average velocity u but rather (4, 5)

$$u' = \frac{\zeta}{\zeta - h} u.$$

One of the most striking results in this case is that the excess velocity $\omega(x)$ is identical to zero everywhere in the inner liquid phase. In order to prove this we introduce the positive definite quantity (13)

$$I \equiv \int_{-\infty}^{+\infty} \eta_{in} \frac{\omega(x)^2}{\zeta(x)} dx = \frac{1}{2\pi} \eta_{ex} \int_{-\infty}^{+\infty} dx \int_{-\infty}^{+\infty} dx' \frac{\omega(x)\omega(x')}{(x-x')^2}. \quad [21]$$

The integral in Eq. [21] is defined again as the Cauchy principal part, and can thus be written as

$$I = -\frac{1}{4\pi} \eta_{ex} \int_{-\infty}^{+\infty} dx \int_{-\infty}^{+\infty} dx' \left| \frac{\omega(x) - \omega(x')}{x - x'} \right|^2. \quad [22]$$

The integrand $[\omega(x) - \omega(x')]/(x - x')$ has no singularity at $x = x'$; thus the integral is well defined and positive. On the other hand, I is itself positive definite, Eq. [21]. It vanishes only if $\omega(x) = 0$, since $\zeta(x)$ is *always positive* for moist wetting. Hence, the only possible value for I is $I \equiv 0$ and thus $\omega(x) = \sigma_{xz}(x) = 0$.

The equation for the profile itself is then

$$\eta_{in} \frac{\zeta - h}{\zeta} u' = -\frac{1}{3} \frac{\partial P}{\partial x} \zeta^2,$$

which has been studied in great detail in Refs. (2, 5, 8) for the liquid/vapor case (neglecting the external phase viscosity).

In summary for the case of moist wetting, the dynamics of spreading is found to be independent of the viscosity of the external liquid, in the limit of small dynamic contact angles. However, note that the disjoining pressure would explicitly depend on the nature of the external liquid. Moreover, we expect this result to hold only for small contact angles.

IV. CONCLUDING REMARKS

The important conclusion of this paper is that even in the limit of *small contact angles*, viscous dissipation in the external liquid phase is extremely difficult to treat exactly. However, our approximated solution suggests that the external phase viscosity plays only a secondary role in this limit; the laws derived for the spreading in the presence of a vapor are still valid with only minor changes.

We would like also to make four additional remarks:

1. The study presented here is limited to small contact angles. To extend it to larger contact angles one would need to solve the hydrodynamic equations in the external liquid phase which, in a first approximation, is a rigid wedge of angle 2α , $\alpha = \pi - \theta/2$. For a wedge bounded by two solid plates, Moffat (12) has shown that if α is smaller than a critical value $\alpha_c \cong 44^\circ$, eddies appear in the flow, and in particular along the bisector plane of the wedge, the velocity varies as $v \sim \sin(\ln r)$. In our problem, the wedge containing the external liquid is bounded by one solid and one liquid boundary. If eddies still exist here, they could change the A/B interface profile. Moreover, they might create corrugations of the interface with dilatational invariance (10). We conjecture that such possible oscillations are important for dynamic contact angles θ_d that are larger than a critical value θ_c (which might depend on the viscosity ratio η_{ex}/η_{in}).

2. When the external liquid is much more viscous than the inner one, there is a small change in the numerical coefficient in Eq. [16] and in Tanner's law, Eq. [1]. However, in front

of the macroscopic wedge, there is an advancing precursor film. We are thus in a geometry where a very thin slab of a less viscous liquid (thickness e) is pushing a more viscous liquid; hence an instability of the Saffman–Taylor-type (11) can appear as shown schematically in Fig. 4. In a Hele–Shaw cell of thickness b and in the limit where $\eta_{in} \ll \eta_{ex}$, all wave vectors smaller than

$$k_c = \frac{1}{b} \left| \frac{12\eta_{ex}u}{\gamma} \right|^{1/2}$$

are unstable. In the spreading liquid case, the restoring force at the contact line can be described by a line tension (2, 14) $\tau \cong \gamma a$, where the equivalent line tension in the Hele–Shaw geometry is γb . One expects all wave vectors smaller than

$$k_c = \left| \frac{12\eta_{ex}u}{e\tau} \right|^{1/2} \quad [23]$$

to be unstable (the role of b is played by the precursor film thickness e).

The instability can develop if both $k_c l \gg 1$ and $k_c \xi \ll 1$, l being the length of the precursor film and ξ being the smallest size on which the film can be distorted (2) (the so-called healing length, $\xi = e^2/a$). If we introduce a characteristic contact angle, $\theta^* = a/e$, and make use of Tanner's law, we find

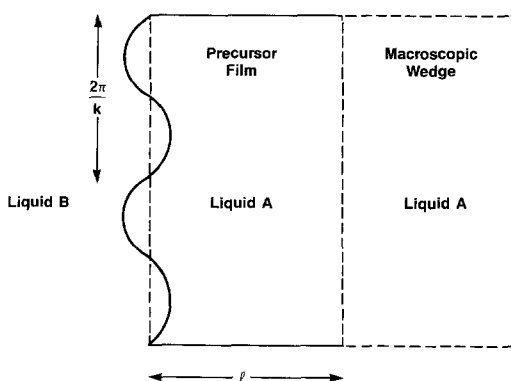


FIG. 4. A schematic top view of the Saffman–Taylor instability at the contact line of a low viscosity liquid pushing a more viscous one on top of a solid surface. The precursor film has a length l and the wavelength of the instability is $2\pi/k$. For a side view see Fig. 1.

$$(k_c l)^2 = \left(\frac{\theta^*}{\theta}\right)^3 \frac{\eta_{ex}}{\eta_{in}} \gg 1,$$

$$(k_c \xi)^2 = \left(\frac{\theta}{\theta^*}\right)^3 \frac{\eta_{ex}}{\eta_{in}} \ll 1. \quad [24]$$

(The inequality signs in Eq. [24] are required for the instability to occur.) When the precursor film exists, $(\theta/\theta^*) \ll 1$, and thus we always have $k_c l \gg 1$. The largest wave vector of an instability is obtained for $k_c \xi \sim 1$. In this case, the wave vector of the instability is

$$k_c = \xi^{-1} \quad \text{if} \quad \frac{\theta}{\theta^*} > \left|\frac{\eta_{in}}{\eta_{ex}}\right|^{1/3},$$

and

$$k_c = \xi^{-1} \left|\frac{\eta_{ex}}{\eta_{in}}\right|^{1/2} \left(\frac{\theta}{\theta^*}\right)^{3/2} \quad \text{if} \quad \frac{\theta}{\theta^*} < \left|\frac{\eta_{in}}{\eta_{ex}}\right|^{1/3}. \quad [25]$$

We note that the Saffman–Taylor instability, which was treated here quite qualitatively, is only one of the plausible instabilities. Another possibility is the pinning of the contact line by impurities on the solid surface (14).

3. We have used crude approximations to study Eq. [14]. A more detailed mathematical treatment is needed in order to get a better solution of this integro-differential equation. Hence, further verification of our solution for the excess velocity $\omega(x)$ is needed.

4. Finally, another special case that was not considered here, but was previously discussed (1), is the dynamics of deposition of a monolayer from a liquid/vapor interface onto a moving solid surface. This is known as a Langmuir–Blodgett film (15), and in this case some of the boundary conditions for the flow

equations are different (1). It will be of interest to further apply our results to this case as well.

ACKNOWLEDGMENTS

We thank P. G. de Gennes for suggesting this problem to us. Some of the derivations presented in this paper are based on his unpublished results. One of us (D.A.) acknowledges the support of the Juliot Curie Fellowship Program.

REFERENCES

- Huh, C., and Scriven, L. E., *J. Colloid Interface Sci.* **35**, 85 (1971).
- For a review see de Gennes, P. G., *Rev. Mod. Phys.* **57**, 827 (1985).
- Brochard, F., and de Gennes, P. G., *J. Phys. (Paris) Lett.* **45**, L579 (1984).
- de Gennes, P. G., and Joanny, J. F., *C.R. Acad. Sci. Ser. 2* **299**, 279 (1984).
- Teletzke, G. F., Davis, H. T., and Scriven, L. E., *Chem. Eng. Comm.*, in press.
- Tanner, L., *J. Phys. D.* **12**, 1473 (1979).
- Hervet, H., and de Gennes, P. G., *C.R. Acad. Sci. Ser. 2* **299**, 499 (1984).
- Joanny, J. F., Thesis, University of Paris VI, 1985. (Unpublished)
- Hardy, H. W., *Philos. Mag.* **38**, 49 (1919).
- Pumir, A., and Pomeau, Y., *C.R. Acad. Sci. Ser. 2* **299**, 909 (1984).
- Saffman, P. G., and Taylor, G. I., *Proc. R. Soc. London Ser. A* **245**, 312 (1958).
- Moffat, K., in "Fluid Dynamics" (R. Balian and J. L. Peube, Eds.). Gordon & Breach, New York, 1973; See also Batchelor, G. K., "An Introduction to Fluid Dynamics." Cambridge Univ. Press, London, 1967.
- de Gennes, P. G., private communication.
- Joanny, J. F., and de Gennes, P. G., *J. Chem. Phys.* **81**, 522 (1984); Joanny, J. F., in "Physics of Finely Divided Matter" (N. Bocarra and M. Daoud, Eds.). Springer-Verlag, Berlin, 1985.
- Blodgett, K., and Langmuir, I., *Phys. Rev.* **51**, 964 (1937); for a recent review see "Langmuir Blodgett Film" (Barlow, Ed.). Elsevier, New York, 1980.